BIVARIATE MOMENT METHODS FOR SIMULTANEOUS COAGULATION, COALESCENCE AND BREAKUP

Dr. R. Bertrum Diemer, Jr., DuPont Engineering Research & Technology, DuPont Company, Wilmington, DE 19898

Prof. Jon H. Olson, Department of Chemical Engineering, University of Delaware, Newark, DE 19716

Abstract

Aerosol reactors pass through regimes where subsets of the population balance terms are dominant. Initially, mixing, reaction, nucleation and accretional growth dominate. This is generally followed by a regime in which coagulation and coalescence control evolution of the particle population into sintered aggregates. Conventionally, the boundary between regimes where coalescence is or is not important is assumed to be sharp and the collision-coalescence regime is followed by a regime dominated by coagulation and breakup which controls the growth of loosely bonded agglomerates that grow large enough to be captured in conventional gas-solids separation equipment. When this boundary is not sharp, there can be a regime in which coagulation, coalescence and breakup all occur simultaneously. This paper describes the daughter distributions required to model breakup in a bivariate population, the moment models describing simultaneous collision, coalescence and breakage, and exhibits reconstructed steady-state distributions formed when the rate kernels are size independent.

Introduction

A scheme for particle formation, growth and transformation is shown in Figure 1. In general, precursor molecules are transformed through some nucleation process into particle nuclei as the initiating event. Additional precursor can add directly to the nuclei causing growth to larger single particles. Particle-particle collisions lead to coagulation into agglomerates. These agglomerates may undergo breakup leading to smaller agglomerates or even back to single particles if conditions are right. It is possible for a steady state to be achieved between coagulation and agglomeration. Although not depicted in the figure, it is possible for precursor molecules to add directly to agglomerates, although that requires the coexistence of unconverted precursor and agglomerated particles. This can be thought of as changing the size of the primary particles in the agglomerate simultaneously with changing the size of the agglomerates. As long as most of the primary particle surface in the agglomerate is accessible for this type of growth, one can think of the nucleation and growth processes as controlling primary particle size and the coagulation and breakage processes as controlling agglomerate size. The population balance problem can be formulated entirely in terms of a single particle size variable, often the particle volume. The problem is said to have one dimension internal to the particle population or to be univariate.

If the primary particle centers in an agglomerate can coalesce so that centers are eliminated, then the combination of collision and coalescence can alter the primary particle size as well. If coalescence is very slow compared to collision, then one has the situation described in the previous paragraph, and the population can be described by one internal dimension. Likewise, if coalescence is very rapid compared to collision then the population can still be described in terms of a single dimension with collisional growth leading to larger single particles. But, when collision and coalescence occur on a similar time scale, then a second internal dimension is needed to describe the population, and the problem becomes bivariate. Typically, the particle surface area is selected as the second internal dimension.

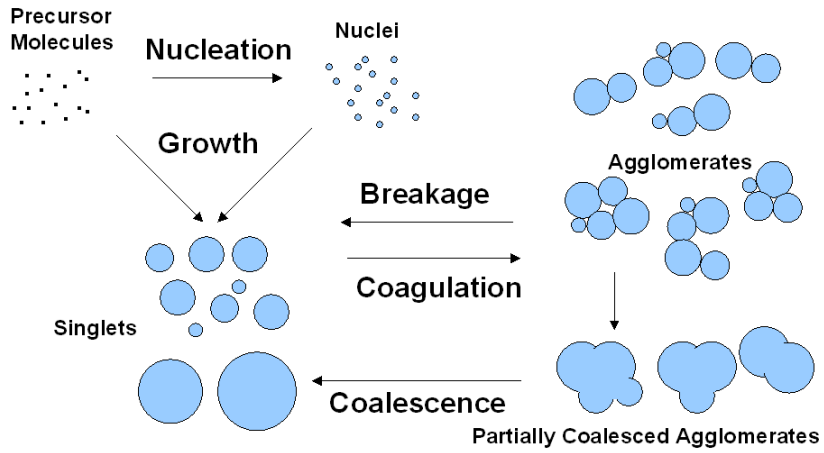

Figure 1: Particle Formation, Growth and Transformation

Figure 2 shows a generic tubular reactor for gas-to-particle conversion. Supposing that the particles are formed by a thermodynamically favored and therefore probably exothermic

process, the temperature profile shown would be likely, with a rise in temperature owing to release of the heat of reaction followed by heat losses or cooling prior to exhausting to a gas-particle separation step. If the reaction is relatively rapid, then reactant mixing, conversion to particle precursor, nucleation and growth all would be occuring as the temperature rose. The full depletion of reactants would correspond to the temperature peak after which no nucleation and accretional growth occur. Although particle-particle collisions can also occur prior to reaching the temperature peak, past this point, the predominant mechanism of particle growth is collisional. If the reactor is hot enough, coalescence occurs simultaneously. For solid particles, the coalescence process is probably solid-state sintering which is known to be sensitive to particle size and temperature such that the coalescence rate can drop rapidly. For this reason, conventional descriptions of aerosol reactor particle formation ([1] through [14]) only consider simultaneous collision and coalescence.

Agglomeration in the absence of coalescence leads to loosely bound flocs that can grow large enough to be broken up by fluid shear. A steady-state size may be reached that sets the requirements for gas-particle separation downstream. Once captured, these particles can be milled to further break up the flocs, so the in-flight floc size is only of interest for sizing the separations equipment [15]. Since the primary particle size is unaffected, the aerosol reactor literature neglects this regime.

Under the right conditions (slow heat removal, rapid collision), an intermediate regime can exist in which agglomerates are coalescing while simultaneously growing large enough to break up under fluid shear. This regime does influence the primary particle size. The models discussed here are developed to describe this regime. It should be noted that the modeling approach also applies in the absence of particle breakage, and as such, broadens the conventional treatment of aerosol reactor particle formation to include this intermediate regime.

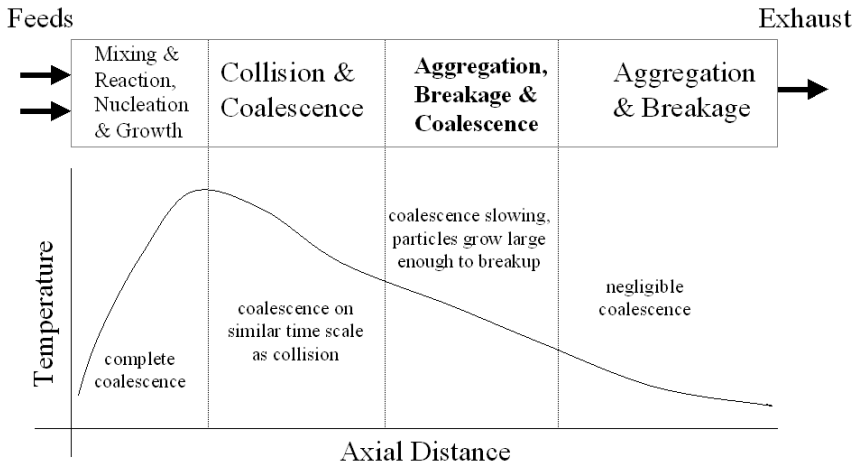

Figure 2: Aerosol Reactor - Dominant Mechanism Schema

For a tubular reactor operating with a nearly uniform velocity profile, the full two-dimensional steady-state population balance equation (neglecting particle diffusion) is given below for

simultaneous coagulation, breakage and coalescence:

$$u\frac{d}{dz}\left[n(V,A)\right] =$$
$$\frac{1}{2}\int_0^V \int_0^A \beta(v, V-v, a, A-a)\, n(v,a)\, n(V-v, A-a)\, dadv$$
$$\underbrace{- n\int_0^\infty \int_0^\infty \beta(v,V,a,A) n(v,a) dadv}_{coagulation}$$
$$\underbrace{+ \int_V^\infty \int_A^\infty \Gamma(\Phi,\alpha)\, b(V,A;\Phi,\alpha)\, n(\Phi,\alpha) d\alpha d\Phi - \Gamma\, n}_{breakage}$$
$$\underbrace{+ \frac{\partial}{\partial A}\left(\sigma(A-A_\infty)n\right)}_{coalescence}$$

In this equation, u is the axial velocity, z is the axial position, n is the particle distribution function in particle concentration units, V is the particle volume, A is the particle surface area, β is the coagulation rate kernel, Γ is the breakage rate kernel, b is the breakage daughter distribution, Φ is the parent particle volume in breakage, α is the parent particle surface area in breakage, σ is the coalescence rate kernel, and A_∞ is the particle surface area at full coalescence.

For the collision-coalescence problem, solution approaches include: full two-dimensional sectionalization ([5], [12], [13], [14]), a reduced sectionalization in the volume dimension alone with calculation of an average surface area for each volume section ([1], [3], [9]), moment models assuming monodispersity in both volume and surface area ([2], [4], [10]), the Quadrature Method of Moments (QMOM)([6],[11]), and Monte Carlo simulation ([7], [8]). Of these, the moment models appear to require the fewest equations and are the most likely candidates for embedding in CFD models of real reactors. In the references cited above, this has actually been done for both monodisperse [2] and QMOM [6] models.

There are two issues associated with moment methods. The first is model closure. The second is distribution reconstruction. A good review of these issues and the various approaches to them for one-dimensional populations can be found in [15], [16] and [17]. The assumption of bivariate monodispersity in [2], [4], and [10] results in a closed moment model that can be solved, but all information about the actual distribution is lost. QMOM models approximate the distribution as a weighted sum of delta functions, allowing the problem to be recast in terms of the weights and locations (abcissas) of the functions. Having the weights and abcissas allows calculation of any desired moment. The methods of distribution reconstruction described in [16] and [17] can be applied to these QMOM-obtained moments as shown in [15]. Another moment method, The Method of Moments with Interpolative Closure (MOMIC), was first suggested by Frenklach and Harris [18], and is further elaborated in [17] and [19]. In this method, a polynomial in the moment order is fit to the natural logs of the known moments, and the missing moments are supplied using the polynomial for interpolation. Distribution reconstructions from this approach are compared to those from QMOM models in [15]. For the test problem studied in [15], it was concluded that models solving 10 moment equations gave reasonable distribution reconstructions whether solved under QMOM or MOMIC closures.

In the following, a bivariate moment model is developed for simultaneous coagulation, breakage and coalescence. The model is closed via MOMIC. An appropriate basis set is developed for extending the one-dimensional reconstruction techniques described in [15], [16] and [17]

to this bivariate problem, and is used to exhibit reconstructed two-dimensional volume-area distributions.

Bivariate Moment Model

The bivariate moment operator is defined as:

$$M_{j,k} = \int_0^\infty \int_0^\infty V^j A^k n\,(V,A)\,dV\,dA$$

Applying this operator to the two-dimensional population balance equation for constant rate kernels, ($\beta = \beta_o$, $\Gamma = \Gamma_o$, $\sigma = \sigma_o$), results in the following set of bivariate moment equations:

$$\frac{dM_{j,k}}{dt} = \frac{\beta_o}{2}\left\{\left[\sum_{n=0}^{j}\sum_{m=0}^{k}\binom{j}{n}\binom{k}{m}M_{n,m}M_{j-n,k-m}\right] - 2M_{0,0}M_{j,k}\right\}$$
$$+ \Gamma_o(b_{j,k}-1)M_{j,k} - k\sigma_o\left(M_{j,k} - \frac{a_o}{v_o^{2/3}}M_{j+2/3,k-1}\right)$$

In this equation, a_o and v_o are the surface area and volume of a fundamental particle (perhaps of the nuclei), and the assumption is that the primary particles retain the same geometry as they grow. Since nucleation and growth are not included as mechanisms, the growth is entirely by coalescence in the scenario under discussion. The quantity $b_{j,k}$ represents the bivariate moment of the breakage daughter distribution which must be specified.

In the absence of coalescence, this set of moment equations would be closed, and could be solved without applying any assumptions or closure rules. In fact, for $k = 0$, one has a moment model for the univariate problem of simultaneous coagulation and breakage under constant kernels. In [16] and [17], a basis set of modified gamma functions is derived from partial analytical solution of this univariate population balance and is applied to reconstruct both steady-state and dynamically evolving univariate distributions under the assumption of various daughter distributions.

Because the missing moments in the above bivariate model are of order $k-1$ in the area index, the moment equations for $k = 1$ can be solved under interpolation of the moments already in hand for $k = 0$. Likewise, the bivariate moments for $k = 2$ can be solved by interpolative closure of the moments with $k = 1$, and so on. In this way, the bivariate model can be solved via MOMIC.

In practice, 10 moment equations were solved for $k = 0$ ($j = 0$ to 9), consistent with the findings in [15] regarding requirements for good univariate distribution reconstruction. To avoid polynomial extrapolation error, only 9 moment equations were solved for $k = 1$ ($j = 0$ to 8) because when $j = 9$, the moment $M_{9+2/3,0}$ is required which is outside the range of moments for the interpolation. Likewise, for $k = 2$, only 8 moment equations were solved ($j = 0$ to 7). This was not a serious problem because only the lower order moments in j at $k = 1$ and $k = 2$ were used for distribution reconstruction.

Therefore, a total of 27 equations was needed for this MOMIC model. Compared to the 561 equations needed for the full two-dimensional sectionalization in [12] or the 66 equations for the reduced sectionalization in [1], this is a much more compact equation set that might successfully be embedded in a CFD simulation. The QMOM model described in [6] and successfully embedded in a CFD simulation required solution of 9 equations. Subsequently

[11], it was shown that a 36-equation QMOM model was more accurate. Based on the findings in [15], it is likely that the same number of equations will be needed to get similar reconstruction accuracies for either MOMIC or QMOM.

Bivariate Distribution Reconstruction

For insight into reconstruction of bivariate distributions, consider the following decomposition of a general bivariate distribution $f(x, y)$ into a marginal-conditional product:

$$f(x, y)dydx \Rightarrow g(x)h(y; x)dydx$$

Letting x designate the size variable, one looks for bounds on the second variable y that are conditional on x. Then one can express y in terms of a displacement w between these bound:

$$y = (1 - w)l(x) + w\,u(x)$$

The factor y^j that will occur in the bivariate moments will become:

$$y^j = \sum_{k=0}^{j} \binom{j}{k} [l(x)]^{j-k} [u(x)]^k w^k (1 - w)^{j-k}$$

The product $w^k(1 - w)^{j-k}$ is in the form of a beta function kernel, suggesting a beta function basis for reconstruction in the w direction.

For the specific problem under discussion, one can work in scaled variables such that:

$$f(x, y)dydx = \frac{n(V, A)dAdV}{M_{0,0}}, \quad x = \frac{V}{V_n}, \quad y = \frac{A}{a_o \left(V_n/v_o\right)^{2/3}}$$

Here, V_n is the number mean diameter equal to $M_{1,0}/M_{0,0}$. The scaling of V by V_n follows the approach in developing similarity variables and solutions followed by Friedlander and co-workers ([20], [21]). The scaling of A is by the surface area of a particle of size V_n at full coalescence.

It can be shown that the bounds on y are:

$$l(x) = x^{2/3}, \quad u(x) = x_o^{-1/3}x, \quad x_o = \frac{v_o}{V_n}$$

where x_o is the scaled value of v_o. The bivariate moments in the scaled variables can be related to the unscaled moments via:

$$\gamma_{j,k} = \int_0^\infty \int_0^\infty x^j y^k f(x, y)dydx = \frac{M_{j,k}}{M_{0,0}(a_o/v_o^{2/3})^k V_n^{j+2k/3}}$$

Using the marginal-conditional decomposition discussed above, and letting the distribution in the displacement variable w be a beta distribution with conditional parameters $a(x)$ and $b(x)$, one can show that these scaled bivariate moments are given by:

$$\gamma_{j,k} = \sum_{n=0}^{k} \binom{k}{n} x_o^{-n/3} \int_0^\infty \frac{B(n + a(x), k - n + b(x))}{B(a(x), b(x))} x^{j+(2k+n)/3} g(x)dx$$

When $k = 0$, this becomes:

$$\gamma_{j,0} = \int_0^\infty x^j g(x) dx$$

which are the moments of the univariate problem for simultaneous coagulation and breakage with constant kernels. As discussed earlier, the function $g(x)$ can be reconstructed from these moments as a sum of modified gamma functions. Therefore, the bivariate moments for orders $k > 0$ contain information on the functions $a(x)$ and $b(x)$. A convenient form for these functions is:

$$a(x) = \exp\left[\frac{a_{-1}}{x} + a_0 + a_1 x\right]; \quad b(x) = \exp\left[\frac{b_{-1}}{x} + b_0 + b_1 x\right]$$

which ensures that they always take on positive values. The constants in the above functional forms are obtained by nonlinear regression against a set of target moments (e.g., $\gamma_{0,1}$,$\gamma_{1,1}$, $\gamma_{2,1}$, $\gamma_{0,2}$, $\gamma_{1,2}$, $\gamma_{2,2}$).

Bivariate Breakage Daughter Distributions

In order to do calculations, it is necessary to define a bivariate daughter distribution for the breakage mechanism. In this section, an approach is described that permits the extent of coalescence of the daughters to "adapt" to the changing extent of coalescence of the parents as measured by the mean value of the displacement variable w.

Following the marginal-conditional decomposition approach discussed in the foregoing, one may decompose the daughter distribution:

$$b(v, a; V, A) = b_v(v; V) b_a(a; v, V, A)$$

In general, the volume and area of the daughters (v, a) is conditional on the volume and area of the parents (V, A). The decomposition says that the volume of the daughter is only conditional on the volume of the parent, and that the area of the daughter is conditional on all three of the other variables.

Much of the breakage literature describes self-similar daughter distributions:

$$b_v(v; V) = \frac{\theta(z)}{V} \quad ; \quad z = \frac{v}{V}$$

The function θ depends only on the daughter-to-parent particle volume ratio. Division by the parent volume V ensures satisfaction of mass conservation in breakage. In [22], it is shown that a generalization of the Hill-Ng power-law product distribution can be used to describe a wide variety of distributions. It also is a beta distribution:

$$\theta(z) = p \frac{z^{q-1}(1-z)^{q(p-1)-1}}{B\left(q, q(p-1)\right)}$$

Here, p is the average number of daughters in a breakage event and the exponent $q-1$ comes from the underlying joint multivariate distribution used by Hill and Ng [23] to derive their distributions for multiparticle breakage assuming statistically indistinguishable daughters. In this case, the underlying joint multivariate distribution is the product of factors z_i^{q-1} each representing the probability of forming a daughter of size z_i.

Extending this to the area dimension, it is hypothesized that the beta function also applies. In the displacement variable w, this is represented as:

$$b_w(w) = \frac{w^{q_a-1}(1-w)^{r_a-1}}{B\left(q_a, r_a\right)}$$

This is termed *beta* breakage. The parameters q_a and r_a could depend on the size x. For simplicity's sake, they were assumed to be independent of size for this study.

If the functions $a(x)$ and $b(x)$ describing the parent distribution are independent of x, then the mean displacement $\bar{w}$ is also independent of x and is equal to:

$$\bar{w} = \frac{\gamma_{j,1} - \gamma_{j+2/3,0}}{\frac{\gamma_{j+1,0}}{x_o^{1/3}} - \gamma_{j+2/3,0}}$$

for all j. For purposes of estimating q_a and r_a, it is assumed that (a) $a(x)$ and $b(x)$ *are* constant and (b) the value of $\bar{w}$ for the daughters is the same as for the parents. The reasonableness of assumption (a) was borne out by subsequent model calculations, showing the near agreement among values of $\bar{w}$ calculated for different orders in volume j. Under assumption (b), the daughters are termed *adaptive*, and in beta breakage, this requires:

$$\bar{w} = \frac{q_a}{q_a + r_a}$$

A well-behaved parameter set satisfying this requirement is:

$$q_a = 1 + \bar{w},\ r_a = \frac{1 - \bar{w}^2}{\bar{w}}$$

The relation at $j = 0$ was used to estimate $\bar{w}$:

$$\bar{w} = \frac{\gamma_{0,1} - \gamma_{2/3,0}}{\frac{\gamma_{1,0}}{x_o^{1/3}} - \gamma_{2/3,0}}$$

All of this connects back to the population balance via the quantity $b_{j,k}$, which for beta breakage is:

$$b_{j,k} = \left(\frac{a_o}{v_o^{2/3}}\right)^k \sum_{n=0}^{k} \binom{k}{n} v_o^{-n/3} \frac{B(q_a + n, r_a + k - n)}{B(q_a, r_a)} \theta_{j+(2k+n)/3} \frac{M_{j+(2k+n)/3,0}}{M_{j,k}}$$

where θ_m is the m^{th} moment in z of $\theta(z)$:

$$\theta_m = \int_0^1 z^m \theta(z) dz$$

Steady-State Solutions

One can show that there are two time scales in this problem, τ_{cb}, the characteristic time for coagulation and breakage and τ_s, the characteristic time for coalescence. In solving the moment models, it is convenient to scale the actual time by τ_{cb} and to define a parameter s in terms of a ratio of characteristic times as shown below:

$$\tau = \frac{t}{\tau_{cb}^{\infty}} = \frac{\beta_o M_{0,0}^{\infty} t}{2} = \Gamma_o (p-1) t, \quad s = \frac{\tau_{cb}^{\infty}}{\tau_s}(p-1) = \frac{\sigma_o}{\Gamma_o} = \frac{2(p-1)\sigma_o}{\beta_o M_{0,0}^{\infty}}$$

In this equation, the superscript $^{\infty}$ refers to the values at steady state. Analysis of the system at steady state reveals that there are two limiting types, depending on the value of s:

(1) coagulation-breakage dominated steady states at small s and (2) coalescence dominated steady states at large s.

As the system approaches full coalescence, the driving force for coalescence goes to zero. Referring to the moment model described in the foregoing, this means:

$$M_{j,k} = \frac{a_o}{v_o^{2/3}} M_{j+2/3,k-1}$$

Applying the relation between these unscaled moments and the scaled moments gives:

$$\gamma_{j,k} M_{0,0} \left(\frac{a_o}{v_o^{2/3}} \right)^k V_n^{j+2k/3} = \frac{a_o}{v_o^{2/3}} \gamma_{j+2/3,k-1} M_{0,0} \left(\frac{a_o}{v_o^{2/3}} \right)^{k-1} V_n^{j+2/3+2(k-1)/3}$$

which reduces to:

$$\gamma_{j,k} = \gamma_{j+2/3,k-1} \Rightarrow \frac{\gamma_{j,k}}{\gamma_{j+2/3,k-1}} = 1$$

at full coalescence. In Figure 3, this ratio is plotted as function of the characteristic time ratio s for various j at $k = 1$ assuming binary uniform (p=2, q=1) adaptive beta daughters. One sees that at large s, these ratios collapses to unity for all j (the moment order in particle volume), indicative of a highly coalesced system. For small values of s, these ratios are greater than unity and split into a spectrum of values in the j index, indicative of dominance by the coagulation and breakage mechanisms.

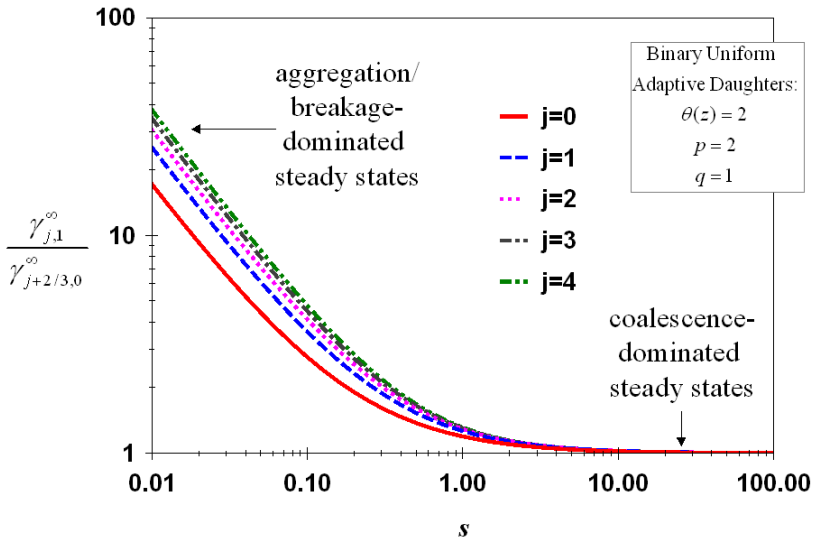

Figure 3: Steady-State Volume-Area Moment Spectra, k=1

As discussed earlier, the mean steady state displacement away from full coalescence can be estimated from the steady state moments. The dependence of this on the characteristic time ratio s is shown in Figure 4 to follow a simple power law that is nearly a direct inverse relationship. One can use this relation to estimate the values of s where coalescence is so rapid or so slow that coalescence may be safely neglected in formulating the population balance. The result is that as long as s is greater than about 1.5 or less than .013, one may neglect the coalescence mechanism in modeling.

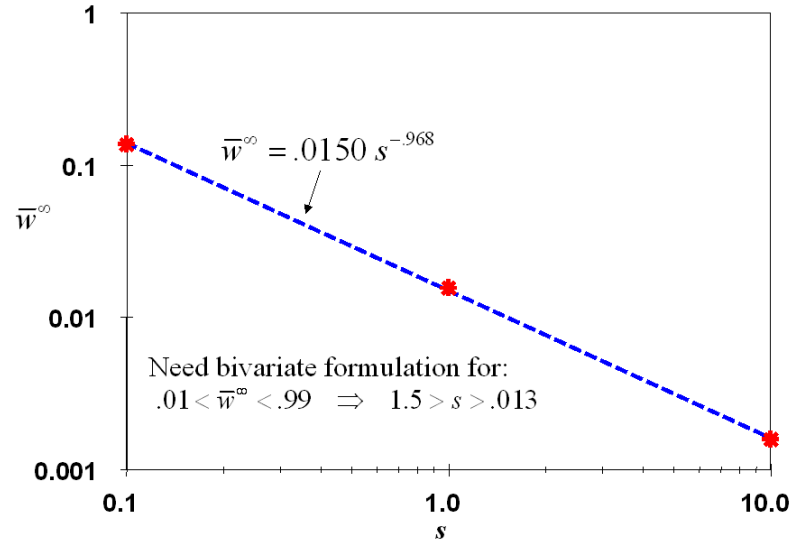

Figure 4: Steady-State Displacement Away from Full Coalescence

Figure 5 shows a reconstructed bivariate volume-area distribution at steady state for slow coalescence ($s = .1$) and binary uniform adaptive beta daughters. The distribution shows that the larger particles are less coalesced than the smaller particles, taking the form of a ridge that arcs from small w-small x to large w-large x values, peaking near $x = 1$. This illustrates the reconstruction capability of the method.

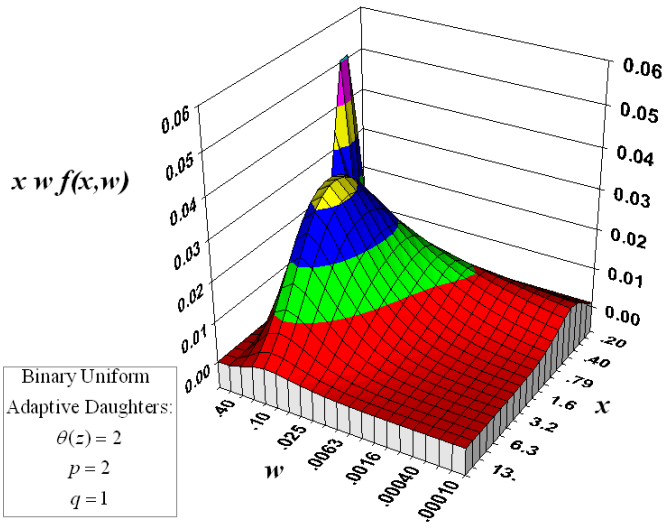

Figure 5: Steady-State Volume-Area Distribution, s=0.1

It is possible to utilize the bivariate moments to estimate primary particle size, or equivalently, the number of primary particles per agglomerate ([24],[25]). This is shown in Figure 6 which is a plot of the primary particle diameter scaled by the diameter corresponding to the

number mean particle volume as a function of the scaled volume variable x. For rapid coalescence, one expects a 1/3-power dependence of this diameter ratio on x, giving a straight line in log-log coordinates. This is exactly what is seen. For the less coalesced systems, the primary particle size is considerably smaller than that for a fully coalesced population. Many powder properties depend on the primary size, and obtaining this type of information is a major motivation for solving this bivariate problem.

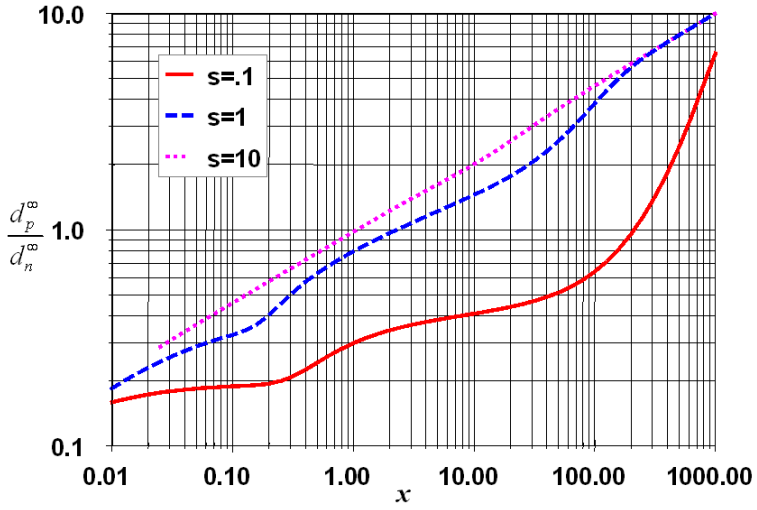

Figure 6: Steady-State Primary Particle Size

Dynamic System Trajectories

Figure 7 shows the dynamic moment trajectories for binary uniform adaptive beta daughters at $k = 0$. At $k = 0$, the coalescence term does not contribute. The system is initialized with a monodisperse distribution of small particles. One sees a rapid development of a metastable moment spectrum that is invariant at scaled times less than unity. Near unity, this transitions to an ultimately stable, time-invariant moment spectrum. What has happened is that early on, the breakage process is a minor contributor because the particles are much smaller than the coagulation-breakage steady-state size. Coagulation under constant kernel has a similarity solution (the exponential distribution, with $\gamma_j = j!$) and this is rapidly achieved as discussed in [17] for initially coagulation dominated systems. As the particles grow large enough for breakage to become important, the system transitions to the coagulation-breakage steady state. This occurs at a scaled time near unity (since the time has been scaled by the characteristic coagulation-breakage time evaluated under steady-state conditions).

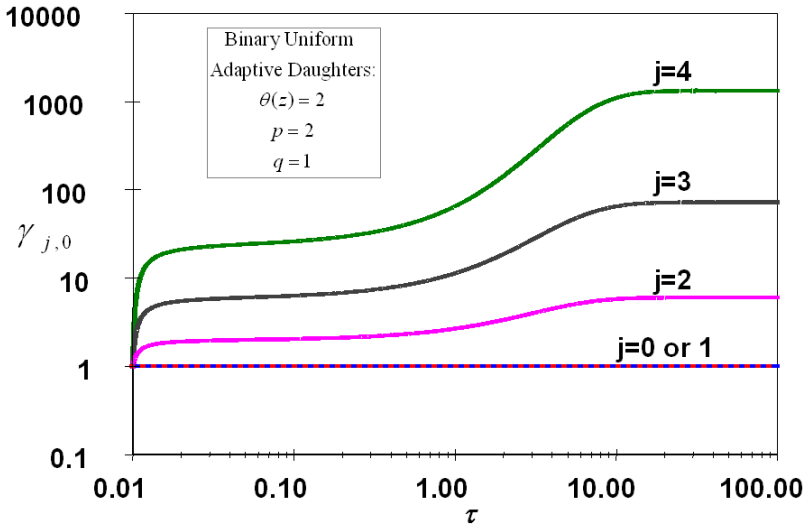

Figure 5: Univariate Moment Trajectories (k=0)

What has happened in Figure 7 is important background for understanding Figure 8, a similar trajectory plot for $k = 1$. On this graph, the trajectories for three different s values are superimposed, representing slowly ($s = .1$), moderately ($s = 1$) and rapidly ($s = 10$) coalescing systems.

For all the systems, the moments rapidly approach an identical set of trajectories representing the increase in area under constant kernel coagulation. From there, the trajectory sets split into three separate ones dependent upon s.

For the slowly coalescing systems, the effect of coalescence is delayed until after achievement of the coagulation-breakage steady state. One sees the transition near scaled time of unity from area growth under constant kernel coagulation to a metastable state corresponding to the coagulation-breakage steady state. Then coalescence kicks in and the moment values are reduced somewhat to the final coagulation-breakage-coalescence steady state. The delayed impact of coalescence means that the system is highly agglomerated and already in a state of dynamic equilibrium between coagulation and breakage when coalescence starts. The steady-state moments are not as low as those at higher values of s, suggesting that surface area is being renewed by the breakage process as quickly as it is being removed by the coalescence process at this steady state. This suggests breakage at relatively small grain boundaries between primary particles rather than primary particle fracture.

For this case, the scaled time at which coalescence kicks in is approximately $\tau = 10$ which is approximately equal to $1/s$. The relation $\tau \approx 1/s$ is equivalent to $t = \tau_s$ meaning that coalescence becomes important when the elapsed time is equal to the characteristic coalescence time. This is the expected result for all values of s.

For the moderately coalescing systems, the overshoot of the final steady state is only exhibited in the lower order moments in j and is attenuated compared to slow coalescence. In the higher order moments in j, the coagulation-breakage-coalescence steady state is smoothly approached. As expected, all of the trajectory adjustment occurs at $\tau \approx 1/s$, which in this

case is near $\tau = 1$.

For the rapidly coalescing systems, the effect of coalescence again kicks in at $\tau \approx 1/s$, which in this case is near $\tau = .1$. The effect of coalescence is to reduce the moment values earlier than the breakage mechanism's impact is seen. The consequence for moments higher order in j is a local minimum near $\tau = 1$ when the effect of breakage increases the area again toward the coagulation-breakage-coalescence steady state. It must be noted that in this scenario, the breakage amounts to more than deagglomeration. It must actually represent primary particle fracture for the moments first-order in area to increase. Whether this is a realistic case is debatable. However, as shown earlier, one would not use a bivariate formulation for systems in which $s = 10$, and one would probably leave out the breakage mechanism unless one could be sure of the existence of a mechanism that would fracture single, highly-coalesced particles.

The three ultimate steady states are different although the moment values for $s = 1$ and $s = 10$ are relatively close to each other compared to those for $s = .1$.

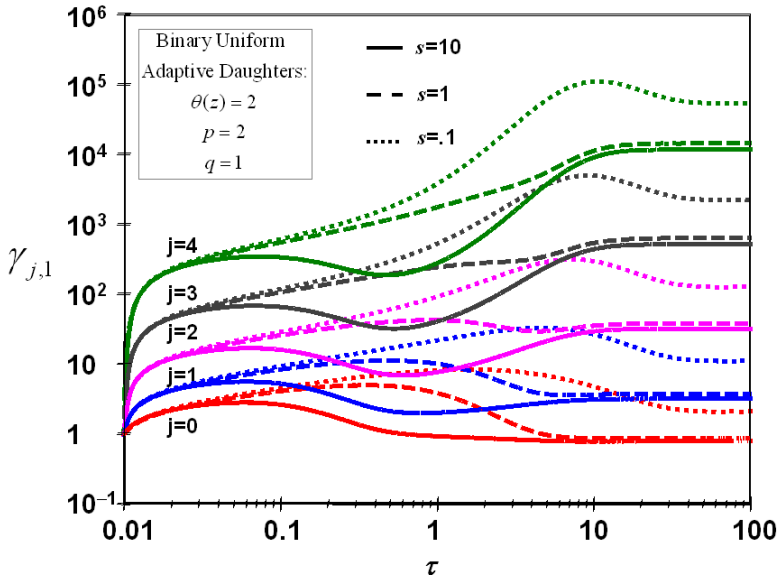

Figure 8: Bivariate Moment Trajectories (k=1)

Conclusions

To recap, a general approach to bivariate problem analysis has been applied to the problem of simultaneous coagulation, breakage and coalescence to extend earlier work on univariate distribution reconstruction to the bivariate problem. This technique starts from the notion of decomposing bivariate distributions into marginal-conditional products, where the marginal distribution is in the size variable and the second variable has bounds conditional on size. This allows access to all of the literature on univariate problems including recent results on distribution reconstruction.

A second transformation of the second variable (in this case surface area) into a displacement between the lower and upper bounds suggests a beta function basis for reconstructing this dimension of the distribution function.

In the present instance, this approach was taken for both the parent aerosol distribution and for the breakage daughter distribution. Beta distributions in a similarity variable are also known to describe univariate breakage and this functionality was extended to the surface area dimension. A means was devised to permit the surface-area-related parameters of the daughter distribution to adapt to the extent of coalescence of the parent distribution.

Moment models based on the MOMIC method were developed for constant rate kernels and solved to obtain both steady-state and dynamic moment sets. The number of model equations (27) was of similar magnitude to other accurate moment models (e.g. 36 equations for the QMOM model in [11]), and substantially smaller compared to either reduced (66 equations) or full (561 equations) two-dimensional sectional models.

Two limiting steady-state types were found, dominated by either (a) coagulation and breakage or (b) coalescence. The steady-state bivariate moments were used to (a) reconstruct full bivariate distributions, (b) relate the mean displacement away from full coalescence to the characteristic time ratio between coalescence and coagulation-breakage, (c) use this relation to estimate when bivariate models are needed, and (d) to calculate the dependence of primary particle size on agglomerate size at steady state.

The dynamic moment trajectories give mechanistic insight by clearly showing the interplay between the three mechanisms when the system is initially dominated by coagulation alone. The transition from the similarity solution for constant kernel coagulation to the coagulation-breakage steady state occurs at times near the characteristic time for coagulation and breakage. Superimposed on this is the impact of coalescence. When the characteristic time for coalescence is much shorter than for coagulation-breakage, coalescence collapses the surface area before breakage kicks in, and any subsequent breakage must reflect primary particle fracture. This is possibly an unrealistic case and in any event, is outside the range of time ratio values (s) where a bivariate formulation is needed. When the characteristic coalescence time is near that for coagulation-breakage, the effect of coalescence is seen during the transition to the coagulation-breakage steady state. When the characteristic time for coalescence is longer than for coagulation and breakage, the effect of coalescence is seen after reaching the coagulation-breakage steady state and can only reduce the surface area partially toward full coalescence because the surface area is continually renewed by breakage along grain boundaries between lightly coalesced primary particles.

References

1. Jeong, J. I., and Choi, M., 2001, A sectional model for the analysis of growth of polydisperse non-spherical particles undergoing coagulation and coalescence, *J. Aerosol Sci.*, **32**, 565-582.

2. Johannessen, T., Pratsinis, S. E., and Livbjerg, H., 2001, Computational analysis of coagulation and coalescence in the flame synthesis of titania particles, *Powder Tech.*, **118**, 242-250.

3. Koch, W., and Friedlander, S. K., 1990, The effect of particle coalescence on the surface area of a coagulating aerosol, *J. Coll. Int. Sci.*, **140** (2), 419-427.

4. Kruis, F. E., Kusters, K. A., Pratsinis, S. E., and Scarlett, B., 1993, A simple model for the evolution of the characteristics of aggregate particles undergoing coagulation and sintering, *Aerosol Sci. Tech.*, **19**, 514-526.

5. Lee, B. W., Jeong, J. I., Hwang, J. Y., Choi, M., and Chung, S. H., 2001, Analysis of growth of non-spherical silica particles in a counterflow diffusion flame considering chemical reactions, coagulation and coalescence, *J. Aerosol Sci.*, **32**, 565-582.

6. Rosner, D. E., and Pyykonen, J. J., 2002, Bivariate moment simulation of coagulating and sintering nanoparticles in flames, *AIChEJ*, **48** (30, 476-491.

7. Rosner, D. E., and Yu, S., 2001, MC simulation of aerosol aggregation and simultaneous spheroidization, *AIChEJ*, **47** (3), 545-561.

8. Tandon, P., and Rosner, D. E., 1999, Monte Carlo simulation of particle aggregation and simultaneous restructuring, *J. Coll. Int. Sci.*, **213**, 273-286.

9. Tsantilis, S., and Pratsinis, S. E., 2000, Evolution of primary and aggregate particle-size distributions by coagulation and sintering, *AIChEJ*, **46** (2), 407-415.

10. Ulrich, G. D., and Subramanian, N. S., 1997, Particle growth in flames III. Coalescence as a rate-controlling process, *Comb. Sci. Tech.*, **17**, 119-126.

11. Wright, D., McGraw, R., and Rosner D. E., 2001, Bivariate extension of the Quadrature Method of Moments for modeling simultaneous coagulation and sintering particle populations, *J. Coll. Int. Sci.*, **236**, 242-251.

12. Xiong, Y., and Pratsinis, S. E., 1993, Formation of agglomerate particles by coagulation and sintering - Part I. A two-dimensional solution of the population balance equation, *J. Aerosol Sci.*, **24** (3), 283-300.

13. Xiong, Y., and Pratsinis, S. E., 1993, Formation of agglomerate particles by coagulation and sintering - Part II. The evolution of aerosol-made titania, silica, and silica-doped titania powder, *J. Aerosol Sci.*, **24** (3), 301-313.

14. Xiong, Y., Pratsinis, S. E., and Weimer, A. W., 1992, Modeling the formation of boron carbide particles in an aerosol flow reactor, *AIChEJ*, (**38** (11), 1685-1692.

15. Diemer, R. B., Jr., and Ehrman, S. H., accepted 2004, Pipeline agglomerator design as a model test case, *Powder Tech.*.

16. Diemer, R. B., and J. H. Olson, 2002, A moment methodology for coagulation and breakage problems: Part 1 - Analytical solution of the steady-state population balance, *Chem. Eng. Sci.*, **57** (12), 2193-2209.

17. Diemer, R. B., and J. H. Olson, 2002, A moment methodology for coagulation and breakage problems: Part 2 - Moment models and distribution reconstruction, *Chem. Eng. Sci.*, **57** (12), 2211-2228.

18. Frenklach, M., and S. J. Harris, 1987, Aerosol dynamics modeling using the method of moments, *J. Coll. Int. Sci.*, **118** (1), 252-261 (1987).

19. Frenklach, M., 2002, Method of Moments with Interpolative Closure, *Chem. Eng. Sci.*, **57** (12), 2229-2239.

20. Friedlander, S. K., and C. S. Wang, 1966, The self-preserving particle size distribution for coagulation by Brownian motion, *J. Coll. Int. Sci.*, **22**, 126-132.

21. Lai, F. S., S. K. Friedlander, J. Pich and G. M. Hidy, 1972, The self-preserving particle size distribution for Brownian coagulation in the free-molecule regime, *J. Coll. Int. Sci.*, **39** (2), 395-405.

22. Diemer, R. B., and J. H. Olson, 2002, A moment methodology for coagulation and breakage problems: Part 3 - Generalized daughter distribution functions, *Chem. Eng. Sci.*, **57** (19), 4187-4198.

23. Hill, P. J., and K. M. Ng, 1996, Statistics of multiple particle breakage, *AIChEJ*, **42** (6), 1600-1611.

24. Diemer, R. B., Jr., and Olson, J. H., submitted 2004, A bivariate methodology for simultaneous coagulation and breakage with coalescence, *J. Aerosol Sci.*.

25. Diemer, R. B., Jr., Moment methods for coagulation, breakage and coalescence problems, Doctoral Dissertation, University of Delaware, 1999.